

Constraints on the $s - \bar{s}$ asymmetry of the proton in chiral effective theory

X.G. Wang^a, Chueng-Ryong Ji^b, W. Melnitchouk^c, Y. Salamu^d, A.W. Thomas^a, P. Wang^{d,e}

^a CoEPP and CSSM, University of Adelaide, Adelaide SA 5005, Australia

^b North Carolina State University, Raleigh, North Carolina 27695, USA

^c Jefferson Lab, Newport News, Virginia 23606, USA

^d Institute of High Energy Physics, CAS, Beijing 100049, China

^e Theoretical Physics Center for Science Facilities, CAS, Beijing 100049, China

Abstract

We compute the $s - \bar{s}$ asymmetry in the proton in chiral effective theory, using phenomenological constraints based upon existing data. Unlike previous meson cloud model calculations, which accounted for kaon loop contributions with on-shell intermediate states alone, this work includes off-shell terms and contact interactions, which impact the shape of the $s - \bar{s}$ difference. We identify a valence-like component of $s(x)$ which is balanced by a δ -function contribution to $\bar{s}(x)$ at $x = 0$, so that the integrals of s and \bar{s} over the experimentally accessible region $x > 0$ are not equal. Using a regularization procedure that preserves chiral symmetry and Lorentz invariance, we find that existing data limit the integrated value of the second moment of the asymmetry to the range $-0.07 \times 10^{-3} \leq \langle x(s - \bar{s}) \rangle \leq 1.12 \times 10^{-3}$ at a scale of $Q^2 = 1 \text{ GeV}^2$. This is too small to account for the NuTeV anomaly and of the wrong sign to enhance it.

Keywords: Strange asymmetry, chiral symmetry, kaon loops

The nature of the quark–antiquark ($q\bar{q}$) sea, which complements the three-valence quark structure of the proton, continues to puzzle and surprise us, as new generations of experiments provide deeper insights into its dynamical origins. From the early simple expectations of a featureless, virtual sea consisting of $q\bar{q}$ pairs generated by gluon radiation in perturbative quantum chromodynamics (QCD), a major paradigm shift occurred with the observation [1, 2, 3, 4] of a predicted [5] large asymmetry between \bar{d} and \bar{u} quarks in the proton. This challenged our traditional view of the nucleon’s peripheral structure, calling into question long held assumptions about the role of nonperturbative physics in understanding the phenomenology of parton distribution functions (PDFs).

With the realization that nonperturbative aspects of QCD were vital for understanding the 5-quark Fock state components of the nucleon light-front wave function [5, 6, 7, 8, 9], an obvious question to ask was whether such effects could lead to other nontrivial features in the $q\bar{q}$ sea. An asymmetry between s and \bar{s} quarks in the nucleon, as anticipated by Signal and Thomas [10], was a natural consequence of SU(3) chiral symmetry breaking in QCD, and speculation later also arose about quark–antiquark asymmetries for charm and heavier quarks [11, 12, 13, 14]. Similar considerations led to questioning the traditional expectations of flavor symmetric polarized sea quarks [15] and even the assumption of charge symmetry in the nucleon PDFs [16, 17, 18].

Apart from its intrinsic interest, the possible strange quark asymmetry, $s - \bar{s}$, is of great importance in connection with its

contribution to the Paschos-Wolfenstein ratio and the NuTeV anomaly [19], which suggested a surprisingly large value for the weak mixing angle, $\sin^2 \theta_W$. A positive value of the integrated difference, or second moment, of the $s - \bar{s}$ asymmetry

$$S^- \equiv \langle x(s - \bar{s}) \rangle = \int_0^1 dx x (s(x) - \bar{s}(x)), \quad (1)$$

of the order $S^- \sim 2 \times 10^{-3}$, along with other corrections such as charge symmetry violation, was found to significantly reduce the excess and bring the NuTeV $\sin^2 \theta_W$ measurement closer to the Standard Model value [20].

Unfortunately, a reliable estimate of the strange asymmetry has been very difficult to obtain. An analysis of early ν and $\bar{\nu}$ deep-inelastic scattering (DIS) data from BEBC, CDHS and CDHSW [21] found a harder s distribution compared with \bar{s} , albeit with a rather large uncertainty, $S^- \approx (2 \pm 3) \times 10^{-3}$. More recent experimental information has come from dimuon production in neutrino-nucleus reactions at Fermilab by the CCFR [22] and NuTeV [23] collaborations, with an NLO analysis finding $S^- = (1.96 \pm 1.43) \times 10^{-3}$ at $Q^2 = 16 \text{ GeV}^2$ [24].

On the theoretical side, calculations based upon fluctuations into meson-baryon Fock components [25, 26, 27, 28, 29, 30, 31, 32] have led to a fairly wide range of predictions, $S^- \sim (-1 \text{ to } +9) \times 10^{-3}$, resulting from the ad hoc assumptions of those models. Clearly, if one is to make reliable predictions for S^- , a more systematic approach is needed, one which has a more direct connection to the underlying QCD theory.

In this Letter we present the first systematic chiral treatment of the $s - \bar{s}$ asymmetry guided by the need to preserve the

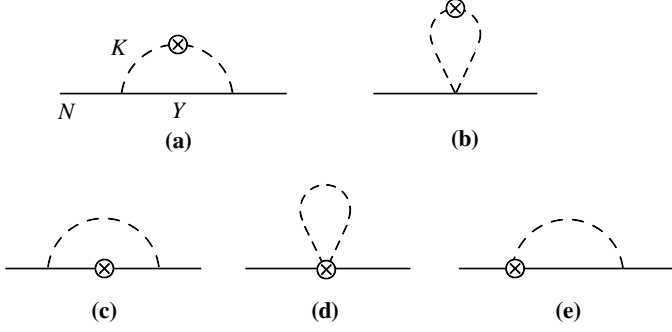


Figure 1: Loop contributions to the \bar{s} PDF from (a) kaon rainbow and (b) kaon bubble diagrams, and to the s -quark PDF from (c) hyperon rainbow, (d) tadpole, and (e) Kroll-Ruderman diagrams. Nucleons N and hyperons $Y = \Lambda, \Sigma$ are denoted by external and internal solid lines, respectively, and kaons K by dashed lines, with crosses \otimes representing insertions of the vector current. The Kroll-Ruderman diagram with a current insertion on the right-hand vertex is not shown.

model independent leading nonanalytic (LNA) behavior of the moments of the strange PDFs. This work builds upon the unambiguous connection between the kaon cloud of the nucleon and QCD which followed the realization [33] that in chiral expansions of moments of strange quark PDFs, the coefficients of the LNA terms in the kaon mass m_K are model independent and can only arise from pseudoscalar meson loops. Starting from the most general effective Lagrangian consistent with the chiral symmetry of QCD, at a given order in the chiral expansion a unique set of diagrams can be identified and computed systematically [34, 35]. The long distance ($m_K \rightarrow 0$) effects in such expansions are thus dictated solely by chiral symmetry and gauge invariance, while the short distance contributions are treated with a particular regularization procedure. The connection with the chiral theory allows us to identify, for the first time, a δ -function contribution to the \bar{s} PDF at $x = 0$, as well as a valence-like component of the s -quark PDF. This result complements earlier discussions of δ -function contributions in the context of the unpolarized Schwinger term and proton spin sum rules [36, 37].

Expanding the chiral SU(3) Lagrangian to lowest order, the complete set of diagrams that contribute to $s - \bar{s}$ is illustrated in Fig. 1. The direct couplings to the kaon loops in Fig. 1(a) and (b) contribute to the \bar{s} PDF, while the s -quark PDF contributions arise from the diagrams involving couplings to hyperons illustrated in Fig. 1(c)–(e). A general feature of the chiral effective theory constrained analyses is the presence of contact terms in Figs. 1(b) and (d) that give rise to contributions at zero kaon light-cone momentum fractions $y = k^+/p^+$, where k is the four-momentum carried by the kaon and p the four-momentum of the proton. These are typically not accounted for in model calculations, which include only the rainbow diagrams in Figs. 1(a) and (c). The Kroll-Ruderman (KR) terms represented in Fig. 1(e) are needed to preserve gauge invariance.

The loop contributions to \bar{s} from the kaon rainbow and kaon bubble diagrams can be written as a standard convolution of nucleon \rightarrow kaon + hyperon splitting functions, $f_{KY}^{(\text{rbw})}$ and $f_K^{(\text{bub})}$,

with the \bar{s} PDF in the kaon,

$$\bar{s}(x) = \left(\sum_{KY} f_{KY}^{(\text{rbw})} + \sum_K f_K^{(\text{bub})} \right) \otimes \bar{s}_K, \quad (2)$$

where the rainbow terms are summed over $KY = K^+\Lambda, K^+\Sigma^0$ and $K^0\Sigma^+$, and the kaon bubble terms over $K = K^+, K^0$, and \otimes denotes the convolution [38, 39], $f \otimes q = \int_0^1 dy \int_0^1 dz f_j(y) q(z) \delta(x - yz)$. The s -quark PDF is also a convolution,

$$s(x) = \sum_{YK} \left(\bar{f}_{YK}^{(\text{rbw})} \otimes s_Y + \bar{f}_{YK}^{(\text{KR})} \otimes s_Y^{(\text{KR})} \right) + \sum_K \bar{f}_K^{(\text{tad})} \otimes s_K^{(\text{tad})}, \quad (3)$$

where $\bar{f}(y) \equiv f(1 - y)$. The hyperon rainbow contributions $f_{YK}^{(\text{rbw})}$ are again summed over all YK combinations, and $f_{YK}^{(\text{KR})}$ are the splitting functions associated with the KR diagrams. The splitting functions for the tadpole diagram, Fig. 1(d), are equal to the $f_K^{(\text{bub})}$ bubble functions from Fig. 1(b). The strange quark hyperon PDFs s_Y , $s_Y^{(\text{KR})}$ and $s_K^{(\text{tad})}$ for the rainbow, KR and tadpole diagrams, respectively, can be related to the u and d PDFs in the proton using SU(3) symmetry.

The splitting function $f_{KY}^{(\text{rbw})}$ in Eq. (2) for the kaon rainbow diagram can be written as a sum of two terms,

$$f_{KY}^{(\text{rbw})}(y) = \frac{C_{KY}^2 \bar{M}^2}{(4\pi f_p)^2} \left[f_Y^{(\text{on})}(y) + f_K^{(\delta)}(y) \right], \quad (4)$$

where $f_Y^{(\text{on})}$ and $f_K^{(\delta)}$ are the on-shell and δ -function contributions, respectively, M (M_Y) are the nucleon (hyperon) masses, $\bar{M} = M + M_Y$, and f_p is the pseudoscalar meson decay constant. The couplings C_{KY} are given in terms of the SU(3) coefficients D and F . The on-shell hyperon piece,

$$f_Y^{(\text{on})}(y) = y \int dk_\perp^2 \frac{k_\perp^2 + [M_Y - (1 - y)M]^2}{(1 - y)^2 D_{KY}^2} F^{(\text{on})}, \quad (5)$$

contributes at $y > 0$, where $D_{KY} \equiv -[k_\perp^2 + yM_Y^2 + (1 - y)m_K^2 - y(1 - y)M^2]/(1 - y)$ is the kaon virtuality for an on-shell hyperon intermediate state, and $F^{(\text{on})}$ is an ultraviolet regulator function. The function $f_K^{(\delta)}$, on the other hand, arises from kaons with $y = 0$,

$$f_K^{(\delta)}(y) = \frac{1}{\bar{M}^2} \int dk_\perp^2 \log \Omega_K \delta(y) F^{(\delta)}, \quad (6)$$

where $\Omega_K = k_\perp^2 + m_K^2$, and $F^{(\delta)}$ is the corresponding regulator. The K bubble diagram in Fig. 1(b) originates with the Weinberg-Tomozawa part of the chiral Lagrangian, and has a distribution, $f_K^{(\text{bub})}$, similar to the δ -function part of the rainbow contribution, but with a normalization that is independent of the SU(3) couplings,

$$f_{K^+}^{(\text{bub})} = 2f_{K^0}^{(\text{bub})} = -\frac{\bar{M}^2}{(4\pi f_p)^2} f_K^{(\delta)}. \quad (7)$$

For the splitting function associated with the hyperon rainbow contribution in Eq. (3) one finds

$$f_{YK}^{(\text{rbw})}(y) = \frac{C_{KY}^2 \bar{M}^2}{(4\pi f_p)^2} \left[f_Y^{(\text{on})}(y) + f_Y^{(\text{off})}(y) - f_K^{(\delta)}(y) \right], \quad (8)$$

where the first (on-shell) and third (δ -function) terms are as in the kaon rainbow contributions, and the hyperon off-shell term is

$$f_Y^{(\text{off})}(y) = \frac{2}{M} \int dk_{\perp}^2 \frac{[M_Y - (1-y)M]}{(1-y)D_{KY}} F^{(\text{off})}, \quad (9)$$

with $F^{(\text{off})}$ the corresponding off-shell regulating function. For the KR contributions in Fig. 1(e), necessary for the preservation of gauge symmetry [40], one has

$$f_{YK}^{(\text{KR})}(y) = \frac{C_{KY}^2 \bar{M}^2}{(4\pi f_P)^2} [-f_Y^{(\text{off})}(y) + 2f_K^{(\delta)}(y)], \quad (10)$$

so that the rainbow and KR contributions satisfy $f_{YK}^{(\text{rbw})} + f_{YK}^{(\text{KR})} = f_{KY}^{(\text{rbw})}$. Finally, the tadpole contribution in Fig. 1(d) is related to the bubble term in Eq. (7), $f_K^{(\text{tad})} = f_K^{(\text{bub})}$. These two conditions guarantee that the net strangeness in the nucleon is zero, $\langle s - \bar{s} \rangle = 0$.

To regulate the ultraviolet divergences in the splitting functions one introduces a regularization procedure, such as a cut-off [39] or a phenomenological form factor [41]. Physically, this takes into account the finite size of the baryon to which the chiral field couples [42, 43]. Here we adopt the Pauli-Villars (PV) method, which preserves the required symmetries and offers many of the advantages of finite range regularization. In this approach one subtracts from the point-like amplitudes expressions in which the propagator mass is replaced by a cut-off mass μ_1 , so that at large momenta the difference between the amplitudes vanishes [44]. For the δ -function term, because both the k^- and k_{\perp}^2 integrations are divergent, a second subtraction, with regulator mass μ_2 , is necessary to render the integrals finite.

For the valence PDFs of the mesons we use the recent fit by Aicher *et al.* [45], assuming

$$\bar{s}_{K^+} = \bar{s}_{K^0} = \bar{d}_{\pi^+}. \quad (11)$$

The strange quark PDFs in the hyperons are related using SU(3) symmetry to the u and d PDFs in the proton,

$$s_{\Lambda} = \frac{1}{3}(2u - d), \quad (12)$$

$$s_{\Sigma^+} = s_{\Sigma^0} = d, \quad (13)$$

for which we use parametrization of Martin *et al.* [46]. For the KR diagrams, the strange PDFs at the KNY vertex are spin dependent. They arise because the KR term, which is required by gauge invariance in the pseudovector chiral theory, involves pion emission or absorption at the vertex which introduces a $\gamma^+ \gamma_5$ coupling. At leading order, SU(3) symmetry requires that these spin dependent PDFs in the proton are related to the spin-dependent PDFs in the proton,

$$s_{\Lambda}^{(\text{KR})} = \frac{1}{3F + D}(2\Delta u - \Delta d), \quad (14)$$

$$s_{\Sigma^+}^{(\text{KR})} = s_{\Sigma^0}^{(\text{KR})} = \frac{1}{F - D}\Delta d. \quad (15)$$

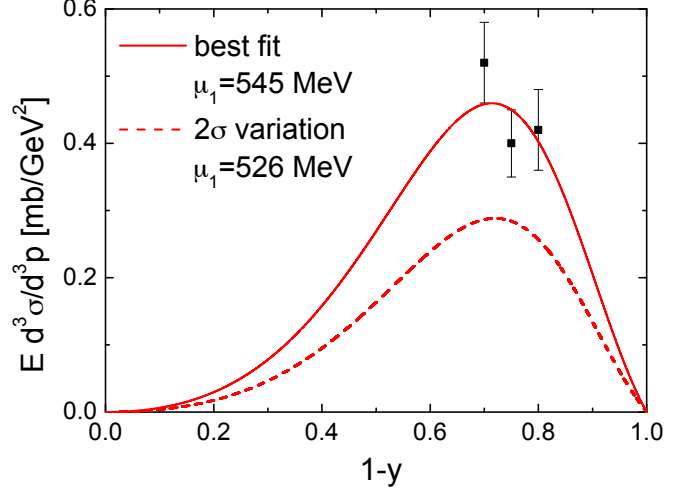


Figure 2: Differential cross section for the best fit to the $pp \rightarrow \Lambda X$ data [49] in the region $y < 0.35$ (solid curve, $\mu_1 = 545$ MeV), as a function of $1 - y$ for $k_{\perp} = 75$ MeV, and for a fit 2σ below the central values (dashed curve, $\mu_1 = 526$ MeV).

The fit from Leader *et al.* [47] is used for both the polarized PDFs and the D and F values to ensure each of the PDFs is normalized to unity. Given the potentially significant violations of SU(3) symmetry found in Ref. [48], we note that there may be corrections to the SU(3) PDF relations (13) – (15) at the 10%–20% level. Finally, for the strange PDF at the $ppKK$ vertex of the tadpole diagram, one has

$$s_{K^+}^{(\text{tad})} = \frac{1}{2}u, \quad (16)$$

$$s_{K^0}^{(\text{tad})} = d. \quad (17)$$

With these relations, the only free parameters in the calculation are the cutoffs μ_1 and μ_2 , which can be constrained phenomenologically.

The ideal process for constraining μ_1 is inclusive Λ hadroproduction, $pp \rightarrow \Lambda X$. At small values of y and k_{\perp} the K exchange contribution in Fig. 1(a) is expected to dominate, while at higher momenta heavier meson and baryon intermediate states, as well as multi meson-exchange processes, will become more important [41].

In Fig. 2 we compare the available bubble chamber data from the CERN proton synchrotron [49] for the lowest available transverse momentum bins. For the differential cross section here the current operator corresponds to the total pK^+ cross section, for which we take the constant value $\sigma_{\text{tot}}^{pK^+} = (19.9 \pm 0.1)$ mb [50]. We find the best fit value for the cut-off $\mu_1 = 545$ MeV, which is taken to yield an upper limit on the kaon contribution. Contributions from non-kaonic backgrounds may reduce this upper limit, although at these kinematics the effect should not be large. As a conservative estimate of the impact of this uncertainty, we also consider the fit that is two standard deviations lower, which corresponds to $\mu_1 = 526$ MeV. These limits yield a range of momentum fractions carried by \bar{s} quarks in the nucleon from $\langle \bar{s} \rangle = 3.4 \times 10^{-3}$ to 5.7×10^{-3} .

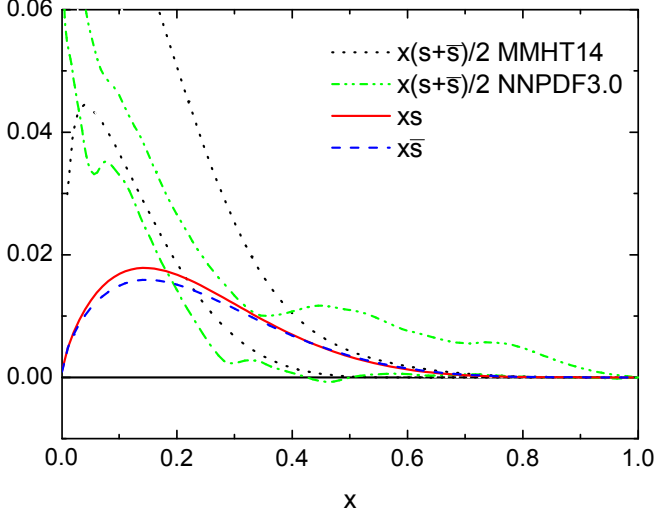


Figure 3: Comparison between the strange xs (solid red curve) and antistrange $x\bar{s}$ (dashed blue curve) PDFs from kaon loops, for the cutoff parameters ($\mu_1 = 545$ MeV and $\mu_2 = 600$ MeV) that give the maximum total $s + \bar{s}$, with the upper and lower limits of the error bands for $x(s + \bar{s})/2$ at $Q^2 = 1$ GeV² from the MMHT14 [51] (black dotted) and NNPDF3.0 [52] (green dot-dashed) global fits.

Because the convolution in Eq. (2) transforms the $y = 0$ contribution in $f_K^{(\delta)}$ to $x = 0$, in practice the \bar{s} distribution will not provide information on the cutoff μ_2 . For the s -quark PDF, since the convolution in Eq. (3) is expressed in terms of the splitting functions evaluated at $1 - y$, the $f_K^{(\delta)}$ contributions here will be transformed to nonzero values of x and appear valence-like. Comparison with the x dependence of the s PDF can then constrain the value of μ_2 .

Our strategy is to fix μ_1 to the maximum value allowed by the comparison with the Λ production data and obtain the corresponding maximum value for μ_2 such that the calculated $s + \bar{s}$ does not exceed the errors on the total phenomenological PDFs, $(s + \bar{s})_{\text{loops}} \leq (s + \bar{s})_{\text{tot}}$. This is illustrated in Fig. 3, where the individual xs and $x\bar{s}$ PDFs from K loops are compared with the recent average $x(s + \bar{s})/2$ parametrization from Refs. [51, 52]. We see that the calculated curves lie below the maximum phenomenological values estimated by both the MMHT and NNPDF collaborations.

For a fixed μ_1 , the allowed range for μ_2 with the PV regularization is $m_K \leq \mu_2 \leq \mu_2^{\text{max}}$. At the preferred value found in Fig. 2, $\mu_1 = 545$ MeV, the upper limit on μ_2 is $\mu_2^{\text{max}} = 600$ MeV. The corresponding range for the strange asymmetry is $-0.07 \times 10^{-3} \leq S^- \leq 0.42 \times 10^{-3}$ at $Q^2 = 1$ GeV². Using the lower value, $\mu_1 = 526$ MeV, reduces the allowed momentum that the s quark can carry, and consequently permits a higher upper limit on μ_2 that still satisfies the constraint in Fig. 3. The limit in this case becomes $\mu_2^{\text{max}} = 894$ MeV, and the range for the strange asymmetry is $-0.01 \times 10^{-3} \leq S^- \leq 1.12 \times 10^{-3}$. Combining these limits, the strange asymmetry for the maximum allowed variations on μ_1 and μ_2 consistent with the available data lies in the range $-0.07 \times 10^{-3} \leq S^- \leq 1.12 \times 10^{-3}$.

For these extremal S^- values, the corresponding shape of

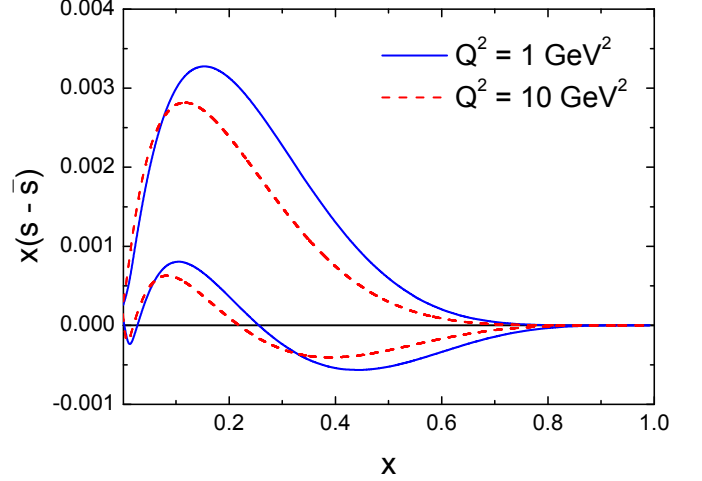


Figure 4: Strange quark asymmetry $x(s - \bar{s})$ at $Q^2 = 1$ GeV² (solid blue curves) and evolved to $Q^2 = 10$ GeV² (dashed red curves). The upper (lower) curves correspond to the maximum (minimum) value for $S^- = 1.12 \times 10^{-3}$ (-0.07×10^{-3}), for cutoff parameters $\mu_1 = 526$ MeV, $\mu_2 = 894$ MeV ($\mu_1 = 545$ MeV, $\mu_2 = m_K$).

$x(s - \bar{s})$ is displayed in Fig. 4. For $\mu_1 = 526$ MeV, the asymmetry remains positive for all x , peaking at $x \approx 0.15$. Interestingly, for this case there is no zero crossing at $x > 0$; conservation of strangeness is ensured by the presence of the nonzero contributions from the δ -function term $f_K^{(\delta)}$ at $x = 0$. This feature is not present in previous loop calculations based on kaon loops, which include only rainbow diagrams, nor in phenomenological PDF fits. For the parameters that give the minimal S^- value, the $x(s - \bar{s})$ distribution also peaks at $x \approx 0.1$, but has a significantly smaller magnitude. Furthermore, the distribution becomes negative for $x \gtrsim 0.2$, which leads to the strong cancellation with the positive distribution at smaller x .

To assess the impact of these asymmetries on the NuTeV anomaly and the extraction of the weak mixing angle, we fold the calculated distributions with the acceptance functional for the NuTeV data [23]. Varying the μ_1 and μ_2 parameters over their maximally allowed range, we find a correction, $\Delta(\sin^2 \theta_W)$, to the weak angle from the strange asymmetry of $-7.7 \times 10^{-4} \leq \Delta(\sin^2 \theta_W) \leq -6.7 \times 10^{-7}$ at $Q^2 = 10$ GeV². Remarkably, for all acceptable values of the cutoff parameters, the correction $\Delta(\sin^2 \theta_W)$ remains negative. While this has the same sign as that needed to reduce the NuTeV discrepancy, the small numerical values that we find reduce the NuTeV anomaly by less than 0.5σ . Had the S^- contribution been large and negative, it would have enhanced the NuTeV anomaly and further underscored the possibility of physics beyond the Standard Model.

We have also considered contributions to the asymmetry from kaon loops accompanied by decuplet hyperons, such as the Σ^* . Any contribution to S^- from these is tempered by the need to reduce the cut-off for the octet component so that the constraint on $s + \bar{s}$ is still respected. As a result, for the range of PV cutoffs considered here we find the net effect of the decuplet to be rather small. Inclusion of higher mass mesons, such as the strange vector K^* mesons [27, 28], goes beyond the chiral theory framework and these are more naturally treated as short-

distance contributions, which should not be added incoherently to other DIS processes.

The virtue of the current study is that we have for the first time computed the full set of diagrams to lowest order within the effective chiral theory. Our analysis has revealed a new contribution to the \bar{s} PDF proportional to a δ -function at $x = 0$, along with a small but nonzero valence-like component of the strange PDF. No phenomenological global PDF fits currently incorporate this physics, and these may need to be generalized to incorporate more flexible parametrizations that allow for such behavior. With the conservative uncertainties chosen for the parameters, we believe this is the most reliable estimate to date of the chiral correction to the NuTeV extraction of $\sin^2 \theta_W$ from the strange quark asymmetry. Ultimately, $s - \bar{s}$ should be determined empirically and, in the absence of high precision ν and $\bar{\nu}$ data on protons, the best hope for better constraints may lie with the associated production of charm with weak bosons at the LHC [53].

Acknowledgements

We acknowledge helpful discussions with J. T. Londergan at an early stage of this work. This work was supported by the DOE Contract No. DE-AC05-06OR23177, under which Jefferson Science Associates, LLC operates Jefferson Lab, DOE Contract No. DE-FG02-03ER41260, the Australian Research Council through the ARC Centre of Excellence for Particle Physics at the Terascale (CE110001104), an ARC Australian Laureate Fellowship FL0992247 and DP151103101, and by NSFC under Grant No. 11475186, CRC 110 by DFG and NSFC.

References

- [1] M. Arneodo *et al.*, Phys. Rev. D **50**, 1 (1994).
- [2] K. Akerstaff *et al.*, Phys. Rev. Lett. **81**, 5519 (1998).
- [3] A. Baldit *et al.*, Phys. Lett. B **332**, 244 (1994).
- [4] R. S. Towell *et al.*, Phys. Rev. D **64**, 052002 (2001).
- [5] A. W. Thomas, Phys. Lett. B **126**, 97 (1983).
- [6] J. Speth and A. W. Thomas, Adv. Nucl. Phys. **24**, 83 (1998).
- [7] R. Vogt, Prog. Part. Nucl. Phys. **45**, S105 (2000).
- [8] G. T. Garvey and J. C. Peng, Prog. Part. Nucl. Phys. **47**, 203 (2001).
- [9] W.-C. Chang and J.-C. Peng, Phys. Rev. Lett. **106**, 252002 (2011); J.-C. Peng and J.-W. Qiu, Prog. Part. Nucl. Phys. **76**, 43 (2014).
- [10] A. I. Signal and A. W. Thomas, Phys. Lett. B **191**, 205 (1987).
- [11] W. Melnitchouk and A. W. Thomas, Phys. Lett. B **414**, 134 (1997).
- [12] S. Paiva, M. Nielsen, F. S. Navarra, F. O. Duraes and L. L. Barz, Mod. Phys. Lett. A **13**, 2715 (1998).
- [13] T. J. Hobbs, J. T. Londergan and W. Melnitchouk, Phys. Rev. D **89**, 074008 (2014).
- [14] F. Lyonnet *et al.*, JHEP **1507**, 141 (2015).
- [15] A. I. Signal, A. W. Schreiber and A. W. Thomas, Mod. Phys. Lett. A **6**, 271 (1991).
- [16] E. Sather, Phys. Lett. B **274**, 433 (1992).
- [17] E. N. Rodionov, A. W. Thomas and J. T. Londergan, Mod. Phys. Lett. A **9**, 1799 (1994).
- [18] J. T. Londergan, J. C. Peng and A. W. Thomas, Rev. Mod. Phys. **82**, 2009 (2010).
- [19] G. P. Zeller *et al.*, Phys. Rev. Lett. **88**, 091802 (2002).
- [20] W. Bentz, I. C. Cloet, J. T. Londergan and A. W. Thomas, Phys. Lett. B **693**, 462 (2010).
- [21] V. Barone, C. Pascaud and F. Zomer, Eur. Phys. J. C **12**, 243 (2000).
- [22] A. O. Bazarko *et al.*, Z. Phys. C **65**, 189 (1995).
- [23] G. P. Zeller *et al.*, Phys. Rev. D **65**, 111103(R) (2002); 119902(E) (2003).
- [24] D. Mason *et al.*, Phys. Rev. Lett. **99**, 192001 (2007).
- [25] W. Melnitchouk and M. Malheiro, Phys. Rev. C **55**, 431 (1997).
- [26] W. Melnitchouk and M. Malheiro, Phys. Lett. B **451**, 224 (1999).
- [27] F. G. Cao and A. I. Signal, Phys. Lett. B **559**, 229 (2003).
- [28] L. L. Barz, H. Forkel, H. W. Hammer, F. S. Navarra, M. Nielsen and M. J. Ramsey-Musolf, Nucl. Phys. A **640**, 259 (1998).
- [29] J. Alwall and G. Ingelman, Phys. Rev. D **70**, 111505 (2004).
- [30] Y. Ding, R. G. Xu and B. Q. Ma, Phys. Lett. B **607**, 101 (2005).
- [31] M. Wakamatsu, Phys. Rev. D **71**, 057504 (2005).
- [32] T. J. Hobbs, M. Alberg and G. A. Miller, Phys. Rev. C **91**, 035205 (2015).
- [33] A. W. Thomas, W. Melnitchouk and F. M. Steffens, Phys. Rev. Lett. **85**, 2892 (2000).
- [34] D. Arndt and M. J. Savage, Nucl. Phys. A **697**, 429 (2002).
- [35] J.-W. Chen and X. Ji, Phys. Rev. Lett. **87**, 152002 (2001); **88**, 249901(E) (2002).
- [36] D. J. Broadhurst, J. F. Gunion and R. L. Jaffe, Annals Phys. **81**, 88 (1973).
- [37] S. D. Bass, Rev. Mod. Phys. **77**, 1257 (2005).
- [38] M. Burkardt, K. S. Hendricks, C.-R. Ji, W. Melnitchouk and A. W. Thomas, Phys. Rev. D **87**, 056009 (2013).
- [39] Y. Salamu, C.-R. Ji, W. Melnitchouk and P. Wang, Phys. Rev. Lett. **114**, 122001 (2015).
- [40] C.-R. Ji, W. Melnitchouk and A. W. Thomas, Phys. Rev. D **88**, 076005 (2013).
- [41] H. Holtmann, A. Szczurek and J. Speth, Nucl. Phys. A **569**, 631 (1996).
- [42] J. F. Donoghue, B. R. Holstein and B. Borasoy, Phys. Rev. D **59**, 036002 (1999).
- [43] R. D. Young, D. B. Leinweber and A. W. Thomas, Nucl. Phys. Proc. Suppl. **141**, 233 (2005).
- [44] X.G. Wang, C.-R. Ji, W. Melnitchouk, Y. Salamu, A. W. Thomas and P. Wang, arXiv:1610.03333 [hep-ph].
- [45] M. Aicher, A. Schäfer and W. Vogelsang, Phys. Rev. Lett. **105**, 252003 (2010).
- [46] A. D. Martin, R. G. Roberts, W. J. Stirling and R. S. Thorne, Eur. Phys. J. C **4**, 463 (1998).
- [47] E. Leader, A. V. Sidorov and D. B. Stamenov, Phys. Rev. D **82**, 114018 (2010).
- [48] S. D. Bass and A. W. Thomas, Phys. Lett. B **684**, 216 (2010).
- [49] V. Blobel *et al.*, Nucl. Phys. B **135**, 379 (1978).
- [50] B. Povh and J. Hüfner, Phys. Rev. D **46**, 990 (1992).
- [51] L. A. Harland-Lang, A. D. Martin, P. Motylinski and R. S. Thorne, Eur. Phys. J. C **75**, 204 (2015).
- [52] R. D. Ball *et al.*, JHEP **04** (2015) 040.
- [53] S. Alekhin, J. Blümlein, L. Caminadac, K. Lipka, K. Lohwasser, S.-O. Moch, R. Petti and R. Placakyte, Phys. Rev. D **91**, 094002 (2015).